

1

Introduction to Millimeter Wave Antennas

Zhi Ning Chen

Department of Electrical and Computer Engineering, National University of Singapore, Singapore 117583, Republic of Singapore.

1.1 Millimeter Waves

Millimeter waves are regulated by the International Telecommunication Union (ITU) as the electromagnetic waves at the wavelength range of millimeter order, namely, 1–10 mm; the corresponding frequency range is from 30 to 300 GHz, or extremely high frequency (EHF), as listed in Table 1.1. However, the systems operating at the frequencies lower than 30 GHz, such as 24 GHz, are also categorized as millimeter wave (mmW) systems simply because the behaviors of the electromagnetic waves at such frequencies are very similar to those at the defined mmW frequencies. Furthermore, the waves at the wavelength of sub-millimeter order, namely 0.1–1 mm, or the frequency range from 300 to 3000 GHz, are regulated as “terahertz (THz) wave,” and the waves at the wavelength of 1 mm–1 m, or the frequency range from 300 MHz to 300 GHz, are regulated as “microwave” by ITU [1]. Therefore, the mmW band is located at the upper edge of the microwave band. Accordingly, the wavelengths at the mmW bands are shorter than those at lower microwave bands but longer than those at infrared bands.

The majority of existing wireless communication and radar systems have been long operating at the lower microwave bands. This book will focus on the waves over the mmW bands at the frequency range from 24 to 300 GHz for wireless applications.

1.2 Propagation of Millimeter Waves

The high frequencies or short wavelengths of the mmWs make their propagation characteristics very unique. The propagation characteristics directly determine the behaviors of waves propagating to desired destinations through a certain path and media. In a long-distance wireless communication, radar, or imaging/sensing application, the propagation properties of the wave fully determine the system design requirements, in particular the selection of the adequate operating frequency and bandwidth [2].

As shown in Table 1.2, the dominant propagation modes of the waves vary against operating frequencies. Furthermore, the types of propagation modes determine the distance of wave propagation. It can be found that:

1. the wave mainly propagates in ionospheric modes like a *skywave* when the frequencies are lower, for instance, at very high frequency (VHF) and below;

Table 1.1 Allocation of the radio frequency bands by ITU.

ITU band number	Designated band	Frequency	Wavelength in air
1	Extremely low frequency (ELF)	3–30 Hz	9993.1–99 930.8 km
2	Super low frequency (SLF)	30–300 Hz	999.3–9993.1 km
3	Ultra low frequency (ULF)	300–3000 Hz	99.9–999.3 km
4	Very low frequency (VLF)	3–30 kHz	10.0–99.9 km
5	Low frequency (LF)	30–300 kHz	1.0–10.0 km
6	Medium frequency (MF)	300–3000 kHz	0.1–1.0 km
7	High frequency (HF)	3–30 MHz	10.0–100.0 m
8	Very high frequency (VHF)	30–300 MHz	1.0–10.0 m
9	Ultra high frequency (UHF)	300–3000 MHz	0.1–1.0 m
10	Super high frequency (SHF)	3–30 GHz	10.0–100.0 mm
11	Extremely high frequency (EHF)	30–300 GHz	1.0–10.0 mm
12	Tremendously high frequency (THF or THz)	300–3000 GHz	0.1–1.0 mm

Note:

1. Hz: hertz
2. k: kilo (10^3), M: mega (10^6), G: giga (10^9), T: tera (10^{12}).

2. the wave can propagate in surface modes like a *groundwave* when the frequencies are at low frequency (LF) to high frequency (HF) bands; and
3. at higher frequencies, typically VHF and above, the wave just travels in direct modes, that is, the *line-of-sight (LOS)*, where the propagation is limited by the visual horizon up to about 64 km on the surface of the earth.

The LOS refers to the waves directly propagating in a line from one transmitting antenna to the receiving antenna. However, it is not necessary for the wave to travel in a clear sight path. Usually, the wave is able to go through buildings, foliage, and other obstacles with diffraction or reflection, in particular at lower frequencies such as VHF and below.

On the other hand, like a light wave, also an electromagnetic wave, the mmWs with shorter wavelengths in millimeter orders, in particular, at EHF and above, always propagate in LOS modes. Their propagation is significantly affected by the typical phenomena of reflection, refraction, diffraction, absorption, and scattering so that a clear path without any lossy or/and wavelength comparable obstacles in the traveling path is required. Such a propagation feature of waves will be reflected in the design considerations of antennas in mmW systems.

Besides the blocking of obstacles in the traveling path, the propagation of the mmWs are also affected by the interaction between the waves and the medium, for example, the atmosphere on the earth. Figure 1.1 shows the average atmospheric absorption of the waves at sea level (i.e., a standard atmospheric pressure of 1013.24 millibar), a temperature of 20 °C, and a typical water vapor density of 7.5 g m^{-3} [3]. The absorption is frequency dependent and ignorable when the frequency is lower than, for instance, 20 GHz with an attenuation less than 0.1 dB km^{-1} or 50 GHz with an attenuation less than 1.0 dB km^{-1} . This is one of the key reasons that almost all existing long-distance wireless systems operate at lower frequencies, for instance, sub-6 GHz bands.

Table 1.2 Dominant propagation modes and typical applications of electromagnetic waves at various frequencies.

Frequency	Wavelength in air	Dominate propagation modes	Typical applications
Extremely low frequency (ELF): 3–30 Hz	9993.1–99 930.8 km	Guided between the Earth and the ionosphere	Very long-distance wireless communication (under water/ground)
Super low frequency (SLF): 30–300 Hz	999.3–9993.1 km	Guided between the Earth and the ionosphere	Very long-distance wireless communication (under water/ground)
Ultra low frequency (ULF): 300–3000 Hz	99.9–999.3 km	Guided between the Earth and the ionosphere	Very long-distance wireless communication (under water/ground)
Very low frequency (VLF): 3–30 kHz	10.0–99.9 km	Guided between the Earth and the ionosphere	Very long-distance wireless communication (under water/ground)
Low frequency (LF): 30–300 kHz	1.0–10.0 km	Guided between the Earth and the ionosphere; ground guided	Very long-distance wireless communication and broadcasts
Medium frequency (MF): 300–3000 kHz	0.1–1.0 km	Ground guided; refracted wave in ionospheric layers	Very long-distance wireless communication and broadcasts
High frequency (HF): 3–30 MHz	10.0–100.0 m	Ground guided; refracted wave in ionospheric layers	Very long-distance wireless communication and broadcasts
Very high frequency (VHF): 30–300 MHz	1.0–10.0 m	Line-of-sight refracted in ionospheric	Wireless communication, radio, and television broadcasts
Ultra high frequency (UHF): 300–3000 MHz	0.1–1.0 m	Line-of-sight	Wireless communication, television broadcasts, heating, positioning, remote controlling
Super high frequency (SHF): 3–30 GHz	10.0–100.0 mm	Line-of-sight	Wireless communication, direct satellite broadcasts, radio astronomy, radar
Extremely high frequency (EHF): 30–300 GHz	1.0–10.0 mm	Line-of-sight	Wireless communication, radio astronomy, radar, remote sensing, energy weapon, scanner
Tremendously high frequency (THF): 300–3000 GHz	0.1–1.0 mm	Line-of-sight	Radio astronomy, remote sensing, imaging, spectroscopy, wireless communications

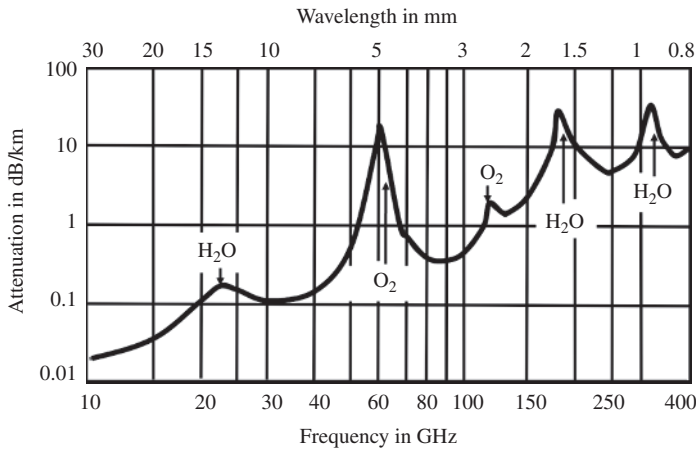


Figure 1.1 The average atmospheric absorption of waves at a sea level at the temperature of 20 °C, standard atmospheric pressure of 1013.24 millibar, and a typical water vapor density 7.5 g m^{-3} [3].

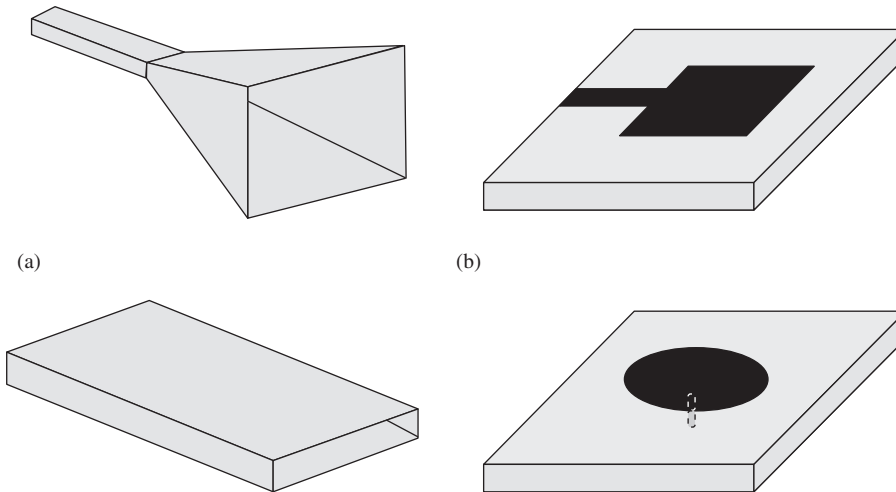


Figure 1.2 (a) Aperture antennas and (b) microstrip antennas.

The wave attenuation is caused by the absorption of water (H_2O) and/or oxygen (O_2) in the atmosphere. There are several absorption peaks across the frequency band up to 400 GHz. The lowest two peaks appear around the 25 and 60 GHz bands, respectively. In particular, the attenuation at the 60 GHz band is 10 times that of the 30 GHz band. In addition, the temperature, pressure, and water vapor density also significantly affect the absorption. It suggests that the wave attenuation at the mmW bands may increase greatly when it is raining, snowing, or foggy. Such an observation must be considered in the calculation of link budget of mmW systems. As a result, the selection and design of antennas should meet the requirements of mmW systems with particular attention to uniqueness of wave propagation.

1.3 Millimeter Wave Technology

1.3.1 Important Features

mmW technology has long been developed for various wireless systems in the past decades because of the apparent advantages over the systems operating at the lower frequency bands, that is, their shorter operating wavelength and wider operating bandwidth with the same fractional bandwidth. The shorter operating wavelength is, for instance, good for an imaging system with higher spatial resolution. Physically the resolution limitations in an imaging system restrict the ability of imaging instruments to distinguish between two objects separated by a lateral distance less than approximately half an operating wavelength of waves used to image the objects.

With the shorter operating wavelengths, mmW systems also enjoy an advantage over the systems operating at lower frequencies, namely, a tiny component size. In particular, the overall volume of the mmW devices can be greatly reduced because the performance of some key radio frequency (RF) components are determined by the electrical size of the design, for instance, antennas and filters. The smaller size of the RF components definitely benefits the device design significantly, especially for applications requiring tiny devices such as handsets, wearables, and implants. For example, it is very challenging to install more antennas, typically more than two antennas operating at the bands of 690–960 MHz in existing handsets with limited overall space. However, it is easy to install multiple antennas and even arrays operating at, for example, 28 or 39 GHz bands for the mobile phones in future fifth generation (5G) networks.

Another attractive advantage is the wide operating bandwidth of the mmW systems. The 10% operating bandwidth at a 60 GHz band offers a bandwidth of 6 GHz, 10 times the 10% bandwidth at 6 GHz, namely 600 MHz. The wider absolute operating bandwidth is able to support the transmission at much higher data-rates according to the Shannon–Hartley theorem. The fundamental information theory tells us that the maximum transmission rate or capacity over a communication channel in the presence of noise is directly proportional to a specified bandwidth [4]. Therefore, the mmW wireless communications can easily achieve the data-rate of a few gigabits per second (Gbps).

1.3.2 Major Modern Applications

The mmW technology has a long history in wireless applications since 1890, Hertz's days [5]. Selected key milestones of mmW research and technology development are briefed in Table 1.3.

With the rapid development of materials, processing, fabrication, and measurement at mmW bands, the mmW technology has been fast applied in modern wireless communications, radar, imaging scanning, and imaging systems. The following sections provide recent examples of new applications of mmW technology.

1.3.2.1 Next-Generation Wireless Communications

Wireless communications are rapidly progressing toward high data-rate and ultra-low latency for the Internet of Things (IoT). Due to the requirement to support higher data-rate, mmW technology is promising for 5G networks over the frequency range from 24 to 86 GHz. Investment on the research and technology development of mmW cellular mobile networks and WLAN/WiFi infrastructures is increasing exponentially. For instance, mmW technology is the main candidate for the

Table 1.3 Selected key milestones of research and development of mmW technology by 1980s.

Period	Important activities	Typical applications	Selected references
1890–1945	<ul style="list-style-type: none"> ● Hertz and Lebedew’s experiments in centimeter / millimeter wavelength ● Nichols, Tear, and Glagolewa-Arkadiewa developed instruments extended to 0.22 and 0.082 mm using spark-gap generator ● Cleeton and William developed vacuum tube sources ● Boot and Randall developed cavity magnetron for radar 	<ul style="list-style-type: none"> ● Confirmed Maxwell’s prediction ● Radiometer ● mmW sources ● 10 and 24-GHz radar 	[5–10]
1947–1965	<ul style="list-style-type: none"> ● Atmospheric attenuation measurement by Beringer, Van Vleck’s and Gordy ● All circular-electric mode transmission with all RF components by Bell Labs ● Geodesic lens antenna by Georgia Technology ● 58-GHz broad-brand helix traveling-wave amplifiers by Bell Labs ● 150-GHz backward-wave oscillators by Thomson-CSF, France ● Imaging line, its associated components and surface-wave propagation on Goubau line or Sommerfeld wave on uncoated metal wire by Wiltse ● First IRE Millimeter and Sub-millimeter Conference held in Orlando, FL, USA in 1963 ● First special issue of The IEEE Proceedings published in April 1966 	<ul style="list-style-type: none"> ● Point-to-point transmission ● The first 14-km long transmission system ● Spectroscopy ● 70-GHz radar ● mmW sources ● High-power mmW sources 	[11–17]
1965–1984	<ul style="list-style-type: none"> ● Development of components at 35, 94, 140, and 220-GHz by US Army Ballistic Research Laboratory as well as Royal Radar Establishment, UK ● The first special issue of the IEEE Transaction on Antennas and Propagation about millimeter wave antennas and propagation. ● Solid state source 	<ul style="list-style-type: none"> ● Radiometers ● Radars ● Missile guidance ● Communications 	More details can be found at [18–20]

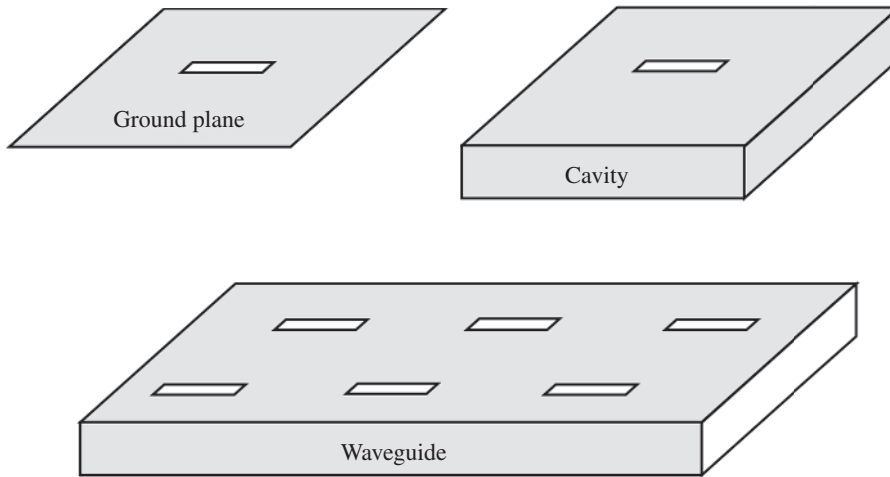


Figure 1.3 Slot antennas.

concept of small cells for future cellular network implementation. The mmW technology can be used not only for mobile terminals but also for point-to-point backhauls, to some degree to replace traditional fiber optic transmission lines by connecting mobile base stations (BSs).

1.3.2.2 High-Definition Video and Virtual Reality Headsets

The transmission of 1080p high-definition (HD) video needs the data-rate up to gigabits per second. None of the existing wireless microwave links can support such high speed at any sub-6 GHz bands. The 60-GHz mmW technology operating, for instance, with unlicensed bandwidths up to 5–7 GHz (for example, US: 57.05–64 GHz and Europe: 57.0–66.0 GHz) can be used to transmit HD video from digital set top boxes, laptops, digital video disc (DVD) players, HD game stations, and other HD video sources to HD television (TV) wirelessly. Furthermore, small transmission devices can be integrated into TV sets invisibly.

Similar to the HD video applications scenarios, virtual reality (VR) applications need ultra-high data-rate wireless links in a short range for future multimedia applications. The wireless links will support the high-speed transmission of video and audio data from mobile devices such as headsets to controlling computers or other VR devices. The mmW wireless communications are the only solution to meet such requirements so far.

1.3.2.3 Automotive Communications and Radars

The mmW radar operating at 24 GHz may be the first mmW system in the history of mmW technology, as shown in Table 1.3. Recently, autonomous driving is being developed very fast. Such applications require the ultra-high-resolution detection of pedestrians and other obstructions as well as communication with other vehicles through the network in real time and low latency. Ultra-high-resolution radars have been developed with the mmW radar systems operating at a range from 77 to 81 GHz. The detection range varies from 0.15 to 200 m. The communications can be built up to achieve the gigabits per second links through 5G networks.

1.3.2.4 Body Scanners and Imaging

Due to the short wavelength for possible high-resolution images and high frequency for fast imaging, the mmW technology has been extensively applied in human body scanners currently in the market. The mmW body scanners have achieved high-precision scanning with much less harm

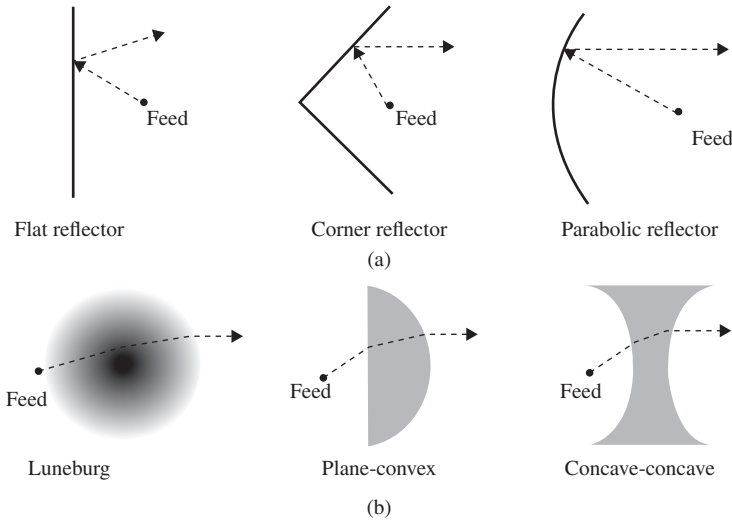


Figure 1.4 (a) Reflector antennas and (b) lens antennas.

to the human body. In particular, such mmW full-body scanners have been very popular for airport security. They use the transmitted power of less than 1 mW and operate at a frequency range between 70 and 80 GHz.

In conclusion, with its unique features, the mmW technology has a very promising future in the applications of high-speed wired/wireless communications as well as radar detection and imaging.

1.4 Unique Challenges of Millimeter Wave Antennas

An antenna is the only means to transfer the electric power from the circuits of a wireless system to a medium and vice versa. There have been many design challenges for conventional antennas such as wide operation bandwidth, high gain and radiation efficiency, desired radiation performance, small/compact size and conformal shapes, and low-cost material utilization and fabrication. However, the design of antennas for mmW systems faces unique challenges because of its higher frequencies, or shorter wavelengths.

From the design point of view:

1. **Wide Bandwidth:** At mmW bands, usually we enjoy wide available spectra for wireless communications and radar applications. The typical operating bandwidth is more than 10% for both required impedance matching and desired radiation performance such as radiation patterns, radiation efficiency, and polarization. It is indeed challenging for the antennas to meet all design requirements simultaneously.
2. **High Gain:** Due to high operating frequencies, the path-loss in propagation at mmW bands, in particular in rainy, foggy, or snowy weather, becomes much more critical than that at microwave bands. To compensate for the high path-loss, we must design antennas with much higher gain. For example, the gain of the antennas should reach up to 15 dBi for 10 m LOS wireless links at 60 GHz bands for some systems under the IEEE 802.11ad standard.
3. **High Radiation Efficiency:** Due to high operating frequencies, the ohmic losses caused by materials and connections in the design become severe. Usually, the loss of the dielectric and metals increase against frequencies. For instance, FR4 has loss tangents of 0.016 at 1 MHz and

> 0.1 at 16 GHz, respectively. The other loss can be caused by surface waves due to electrically thick dielectric used in antenna design. For instance, the dielectric substrate of a patch antenna increases its electrical thickness from a typical 0.01 operating wavelength at a frequency of 2.4 GHz to 0.1 wavelength at 24 GHz if the same dielectric substrate is used for the patch antenna design. The thicker substrate inevitably causes severer surface waves. The increased surface waves guide part of the radiated power to other directions rather than the desired direction, for instance, boresight. Such loss lowers the radiation efficiency or gain of the antenna.

4. *Beam-Scanning Functionality*: Due to the need of high gain, the beamwidth of the radiation pattern is narrow so that it is difficult to achieve a wide coverage, but it is easy for the radiation to be blocked by unwanted obstacles. To keep propagation links unbroken, the functionality of beam-scanning of antennas is one solution. Therefore, much more expensive and complicated antenna designs are necessary.

From the fabrication and measurement point of view:

1. *High-End Material and Tight Tolerance Fabrication*: To keep low the ohmic loss caused in materials, high-end materials, usually at higher prices, must be used. For instance, FR4 is replaced by more expensive but higher performance Rogers or ceramic or liquid crystal polymer (LCP). Meanwhile, due to the shorter wavelengths at higher frequencies, higher-precision fabrication processes are needed to achieve results within the acceptable tolerance. For example, conventional printed circuit board (PCB) process can guarantee a tolerance of 0.2 mm, which is 0.2% wavelength at 3 GHz but 4% wavelength at 60 GHz!
2. *Testing Setup*: There have been many antenna testing setups up to 40 GHz in the market and laboratories. It is necessary to upgrade the setups and system for the antenna test for the frequencies higher than 40 or 67 GHz. Expensive frequency up-converter heads are necessary for the frequency extension of such mmW systems. For the measurement of impedance or S-parameters, high-quality but expensive connectors and cables must be used to keep the insertion loss acceptable. In addition, the on-wafer mmW antenna measurement must be carried out using precise and expensive probes where the measurement is usually conducted on expensive specific probe stations. For the measurement of radiation performance, due to the lack of link budget and the concern of testing environments, it is necessary to design the setup by customizing the mechanical structures with high-precision location and orientation.

In short, the design of mmW antennas faces much more lossy, complicated, and costly issues than those at lower microwave frequencies. The research and development activities of mmW antenna technology should be done by taking all such unique challenges into account.

1.5 Briefing of State-of-the-Art Millimeter Wave Antennas

From an antenna operation point of view, mmW antennas can be any type of radiators, such as wire, aperture, slot, microstrip, reflector, and Lens as shown in Figures 1.2, 1.3, and 1.4. Also the radiators can be arranged as arrays to enhance their radiating performance and achieve more functionalities. However, due to the unique challenges caused by their physically short wavelengths, namely 1 mm at 300 GHz to 10 mm at 30 GHz in free space as mentioned above, some types of radiators are more suitable for mmW antenna designs, as shown in the general discussion listed in Table 1.4. The discussion is based on the basic versions of all types of antenna designs. A variety of variations of the antenna have long been proposed for performance enhancement as presented in the References [21, 22].

Table 1.4 mmW antennas.

Type of radiator	Fabrication/Testing	Performance/Applications	Sketches
Aperture: <ul style="list-style-type: none"> ● Horn ● Open-end waveguide ● Waveguide horn 	<ul style="list-style-type: none"> ● Easy fabrication and test ● Bulky three-dimensional geometry for metal structures ● Difficult to be integrated with circuits ● Low loss for air-filled design ● Possibly fabricated using PCB^{a)} and LTCC^{b)} processes 	<ul style="list-style-type: none"> ● Moderate bandwidth ● High gain ● Point to point link ● Standard antennas in measurement systems 	Figure 1.2
Microstrip patch	<ul style="list-style-type: none"> ● Easy fabrication and test ● Flat and low-profile geometry ● Lossy at high frequencies ● Wide feeding strips ● Conformal configuration ● Easy to form arrays ● Easy to be integrated with circuits ● Easy to be fabricated using PCB and LTCC processes 	<ul style="list-style-type: none"> ● Narrow bandwidth ● Low gain ● Broadside radiation ● Wide applications 	
Slot: <ul style="list-style-type: none"> ● On ground ● On cavity ● On waveguide 	<ul style="list-style-type: none"> ● Easy fabrication and test ● Flat geometry ● Easy to form arrays ● Conformal geometry ● Difficult to be integrated with circuits 	<ul style="list-style-type: none"> ● Narrow bandwidth ● Low gain ● Broadside radiation 	Figure 1.3
Reflector: <ul style="list-style-type: none"> ● Corner ● Flat plane ● Curved plane 	<ul style="list-style-type: none"> ● Not easy fabrication and test ● Bulky and three-dimensional geometry with feed ● Not easy to form arrays ● Difficult to be integrated with circuits 	<ul style="list-style-type: none"> ● Wide bandwidth ● Ultra-high gain ● Directional radiation 	Figure 1.4
Lens: <ul style="list-style-type: none"> ● Luneburg ● Convex-plane ● Concave-plane ● Concave-concave ● Convex-concave ● Convex-concave ● Convex-convex 	<ul style="list-style-type: none"> ● Not easy fabrication but easy test ● Bulky, heavy and three-dimensional geometry with feed ● Not easy to form arrays ● Difficult to be integrated with circuits 	<ul style="list-style-type: none"> ● Wide bandwidth ● Ultra-high gain ● Directional radiation 	
Wires and their variations on substrate	<ul style="list-style-type: none"> ● Easy fabrication and test ● Flat and low-profile geometry ● Lossy at high frequencies ● Wide feeding strips ● Conformal configuration ● Easy to form arrays ● Easy to be integrated with circuits ● Easy to be fabricated using PCB and LTCC processes 	<ul style="list-style-type: none"> ● Moderate bandwidth ● Low gain ● Broadside/endfire radiation 	

a) PCB: printed circuit board.

b) LTCC: low-temperature co-fired ceramic.

Also the antennas can be categorized into two classes based on physical geometry: flat/planar and three-dimensional structures. For high-gain applications, which are always required for mmW systems as mentioned previously, three-dimensional designs such as reflector and lens antennas are perfect options if there is no space and installation constraints; the large-scale arrays of planar elements such as microstrip antenna arrays and slot antenna arrays usually suffer from the difficulty to form the large-scale feeding network in a limited physical space and high loss caused in the feeding networks.

As an alternative, a technique of laminated waveguides on PCB substrate was invented [23, 24], which is to some degree considered the extension of the work based on post-rod to form air-waveguides [25]. Later the structure was comprehensively studied and named as substrate integrated waveguide (SIW) and widely applied in mmW antenna designs [26, 27], where an electromagnetic waveguiding structure is constructed by the two walls formed by two arrays of metalized vias. The spacing between the adjacent vias must meet the criteria to stop the leak of wave propagating in the structure. Such a substrate-integration technology provides much flexibility for waveguide designs and relevant antenna designs, in particular, at mmW bands.

1.6 Implementation Considerations of Millimeter Wave Antennas

At mmW bands, the integration of antennas and substrate by using a multilayer substrate process are desired for planar or flat design of system boards. The substrate integrated antenna (SIA) can be fabricated exactly as a conventional circuit as for printed circuits on layered boards, where the antennas become part of circuit boards or package of integrated circuits. Such integration greatly reduces the loss caused by the connection between the circuits and the antennas, miniaturizes the size of the system, lowers the fabrication cost, and increases the robustness of the system without additional installation of antennas. The integration of the antennas on the substrate is critically determined by fabrication including the selection of substrate materials and the applicable fabrication process.

1.6.1 Fabrication Processes and Materials of the Antennas

With the shorter operating wavelengths in the order of a millimeter, the fabrication of mmW antennas needs a tolerance usually tighter than microwave to achieve the desired performance. For example, for a straight thin half-wave dipole antenna operating at 60 GHz, the overall length of the antenna is about 2.5 mm. The acceptable fabrication tolerance is typically 0.2% wavelength, namely 0.05 mm, which nearly reaches the limit of the conventional commercial PCB process. The tighter tolerance of fabrication is needed if the antennas and feeding network are printed on the PCBs with the relative dielectric constant larger than unit. Therefore, the selection of fabrication for mmW antennas with feeding networks is more critical than that at lower microwave bands, not only because of the tolerance but also costs including processing, materials, and assembling.

At the mmW bands, multilayered substrates such as polytetrafluoroethylene (PTFE), a synthetic fluoropolymer of tetrafluoroethylene, and PTFE composite filled with random glass or ceramic such as RT/duroid® are commonly used for laminating circuits and antennas. PTFE-based substrates usually feature a low and stable loss tangent typically of 0.0018 at 10 GHz and even higher and high resistance to chemical processing and are waterproof and thermally stable. PTFE-based substrates, however, suffer from a higher cost compared to FR4 glass epoxy, are softer materials, and have a higher thermal expansion coefficient. FR4 glass epoxy is most commonly used in frequencies lower than 3 GHz because of its increasing loss tangent against frequency.

LCPs are a class of aromatic polymers. The unique feature of the LCP substrate is its softness although it has similar properties to PTFE-based substrates such as extreme chemical resistance, high mechanical strength at high temperatures, and inertness. Its poor thermal conductivity and surface roughness should be taken into account in electrical applications, in particular, at mmW bands.

To meet the requirements of fabrication tolerance, electrical, and other mechanical properties, low temperature co-fired ceramic (LTCC) has long been used as a cost-effective substrate technology in electrical and electronic engineering, especially at higher frequencies. LTCC is a multilayered glass ceramic substrate. It is co-fired with low-resistance metal conductors, such as Au or Ag, at low firing temperatures, usually $\sim 850\text{--}900^\circ\text{C}$, compared with high temperature multilayered ceramic sintered at $\sim 1600\text{--}1800^\circ\text{C}$. There have been many ceramic materials developed by commercial companies. More detailed information can be found in the book [28], which studies a variety of electrical materials for mmW applications. In particular, the information about the ceramic materials used in LTCC is comprehensive.

For example, Ferro A6M has been widely used in applications at mmW bands. It has a relative dielectric constant of 5.9–6.5 and loss tangent of $\sim 0.001\text{--}0.005$ at 3 GHz. In particular, the electrical properties are stable against frequency. The relative dielectric constant and loss tangent of DuPont 951 ceramic are ~ 7.85 and 0.0063 at 3 GHz, respectively. It should be noted that the ceramic used in LTCC usually has the relative dielectric constants of $\sim 6\text{--}10$, sometimes ~ 18 [29]. High relative dielectric constants are usually not desired for antenna design at mmW bands because they will shrink the dimensions of antennas so that the fabrication needs much higher accuracy [30].

With an LTCC process, the LTCC ceramic substrate can host almost an infinite number of layers. The thin layers are stacked one on the top of another. The conducting paths of gold or silver thick film pastes are printed on each surface layer by layer using the silk-screen printing method. When the multilayer setup has been stacked and printed, it is then fired in the process oven where the low sintering temperature allows the use of gold and silver as conducting traces. The simplified description of process includes:

Step I: via punch, via conductor fill, and trace printing;

Step II: layer stack and lamination; and

Step III: layer co-fire.

The PCB and LTCC processes are concisely compared in Figure 1.5. From a waveguide feeding network and antenna design point of view, the most important difference between the PCB and LTCC processes is that the LTCC process is able to implement the blind via and embedded cavity while the PCB process is unable to do it.

Furthermore, the LTCC used for SIA designs also increases the advantages such as low loss tangents, low permittivity tolerance, good thermal conductivity, multilayered substrate, cavities/embedded cavities, low material costs for silver or gold conductor paths, easy integration with other circuits, and low production costs for medium and large quantities.

In our experience, the PCB process is preferred for SIA designs when an operating frequency is lower than 60 GHz, while LTCC is a good candidate antennas operating at frequencies higher than 60 GHz and up to 300 GHz. At frequencies higher than 300 GHz, the LTCC fabrication becomes quite challenging because of its process limit such as via-hole pitch.

1.6.2 Commonly Used Transmission Line Systems for Antennas

Like any antenna systems, their feeding structures will be a critical issue in the implementation of the antenna design. In particular, the losses caused in the feeding networks greatly degrade the

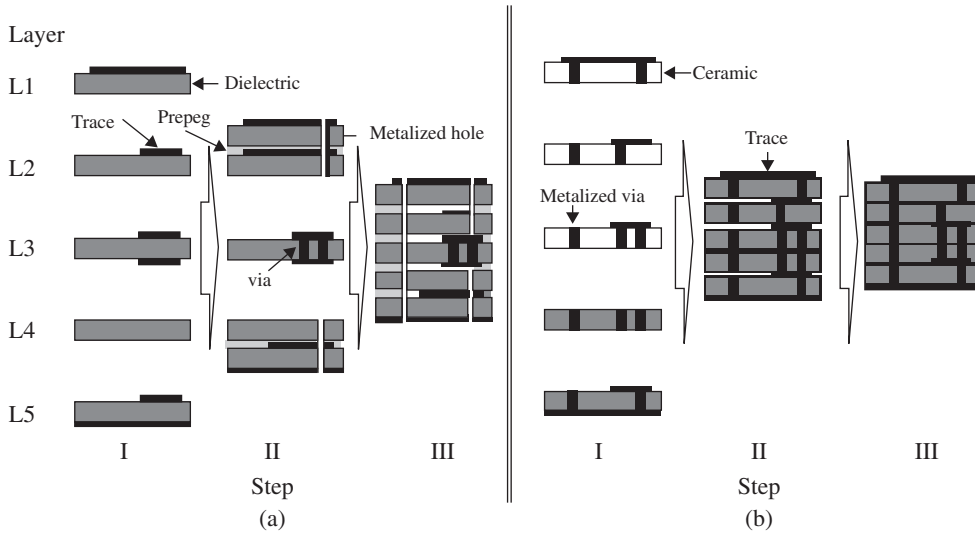


Figure 1.5 Simplified descriptions of PCB and LTCC processes. (a) PCB and (b) LTCC.

performance of the antenna arrays at mmW bands. Unlike the antennas at microwave bands, the losses can be caused by not only the dielectric substrate but also metals used as conductors for transmission and radiation. Like any dielectric at microwave bands, the loss of a dielectric substrate is measured by its loss tangent. Different from the designs at microwave bands, the metal loss that may be caused by the conductivity and surface roughness of the conductors can't be ignored.

Besides microstrip transmission lines, the waveguide-type transmission line systems are popularly used because they may enjoy the lower losses caused by dielectric and metals at mmW bands [23–27, 31]. Accordingly, for instance, the loss analyses have been conducted for microstrip lines, solid-metal-wall waveguides, and post-wall or laminated waveguide or SIW [32]. The study shows that in general the solid-metal-wall waveguides without dielectric loss enjoy less metal loss while microstrip lines suffer from several dielectric losses. The post-wall waveguides or SIWs feature acceptable total losses caused by both dielectric and metal losses at mmW bands. However, it should be noted that the causes of losses of transmission line systems can be complicated because they will be determined by the materials such as dielectric and metals as well as the types or configurations of transmission lines.

The transmission line systems can be in the form of microstrip lines and coaxial lines. Compared with conventional cylindrical versions, the substrate integrated coaxial line (SICL) is a type of planar rectangular coaxial lines. The lines comprise a strip sandwiched between two grounded dielectric layers and laterally shielded by the arrays of metallized vias [33]. Similar to the conventional coaxial line, the propagation of SICL is still in the dominant mode of transverse electromagnetic (TEM).

The SICLs can be realized using a traditional multilayer PCB or LTCC process. Therefore, SICLs feature the combined advantages of the coaxial lines and the planar transmission lines, including the wideband unimodal operation, low cost, non-dispersive performance, good electromagnetic compatibility, and easy integration with other planar circuits. It has been used for high-speed data transmission [34] and various other applications such as antennas, couplers, baluns, and filters at mmW bands [35–41].

Moreover, the substrate integrated gap waveguide (SIGW) or printed ridge gap waveguide (PRGW) is proposed for the transmission line systems at mmW bands. The SIGW or PRGW is the combination of the microstrip-line and gap-waveguide technology based on the PCB or LTCC

process [42–44]. The inverted printed strip line is arranged on or above the periodic mushroom structures where the unwanted surface waves are suppressed and only the quasi-TEM mode is permitted over the operating band. Unlike SIW or SICL, the top and bottom grounds of a SIGW are unconnected. Therefore, the processing complexity is greatly reduced. The SIGW/PRGW technology has been widely used in the antennas and arrays at mmW bands [44–51].

It should be noted that the selection of the materials and transmission line systems significantly affects the antenna efficiency. The loss analyses of antennas including their feeding structures are strongly suggested to understand the main causes of the losses in order to control the overall loss by properly selecting the materials and the types of transmission systems, as well as optimizing the design configurations [52].

1.7 Note on Losses in Microstrip-Lines and Substrate Integrated Waveguides

As previously mentioned, to compensate for the path-loss at higher frequencies, usually very large-scale antenna arrays are required in mmW systems. In such large-scale antenna arrays the feeding network inevitably becomes complicated with a labyrinth of feeding network. The long current or power paths in the network are the critical causes for transmission losses. The additional unignorable transmission losses may be the stopper to limit the achievement of high gain of larger-scale antenna arrays when the insertion loss cancels the increase in the gain by increasing the number of the elements of arrays. For example, if the insertion loss caused by the increase of the power path of the feeding network reaches nearly 3 dB, the antenna array with doubled number of elements will achieve very little gain enhancement. Therefore, it is important to check the transmission line systems in terms of insertion loss before the design of the arrays at mmW bands.

Next, the insertion losses in microstrip-lines (MSLs) and SIWs in LTCC at 60 GHz are compared as an example. The LTCC is Ferro A6-M with relative dielectric constant $\epsilon_r = 5.9 \pm 0.20$, loss tangent $\tan\delta = 0.002$ at 100 GHz. The conductor used for metallization and vias is Au, whose conductivity is $4.56 \times 10^7 \text{ S}\cdot\text{m}^{-1}$.

Figure 1.6 shows a 10-mm long bent MS transmission line on an LTCC board. The 50- Ω MSL is with two ports in the simulation. Figure 1.7 compares the insertion losses for varying thickness of the LTCC board over a frequency range of 0–70 GHz. It is seen that when the thickness increases, the insertion at higher frequency edge quickly increases. For instance, the loss per centimeter reaches up to 13 dB when the thickness is larger than 0.7 mm.

Figure 1.8 clearly shows the causes of the insertion losses at higher frequencies or mmW bands. The losses caused by the dielectric substrate and conductor in the system are just a small percentage of the total losses. It is believed that at 60 GHz, the higher-order modes excited by the discontinuity of the MS cause large surface wave (SW)/leaky losses as previously discussed. This issue is even severer for the thicker substrate. So the SW of MS at mmW is definitely a big problem for practical antenna design.

Figure 1.9 shows a 10-mm long bent SIW in an LTCC board. Figure 1.10 shows the main losses at 60 GHz of a bent SIW in an LTCC board with varying thickness. It is clear that on the contrary, the SIW system does not suffer from such a dilemma, with the highest loss less than 1 dB per centimeter at smaller thicknesses and total losses lower than 0.6 dB for a thickness larger than 0.3 mm. The low-loss feature is quite stable for all the thicknesses. But actually for the very thin thickness of 0.1 mm, the conductor loss is high for the SIW. Fortunately, the thickness of 0.5 mm is usually selected for SIW at 60 GHz. In particular, the majority of losses are caused by both the dielectric and conductors, which is different from the MS lines.

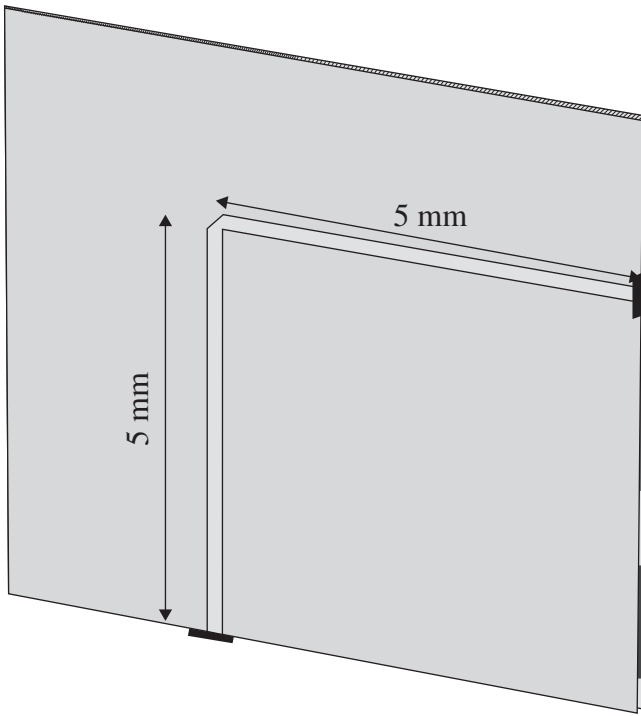


Figure 1.6 A bent MS transmission-line on a LTCC board.

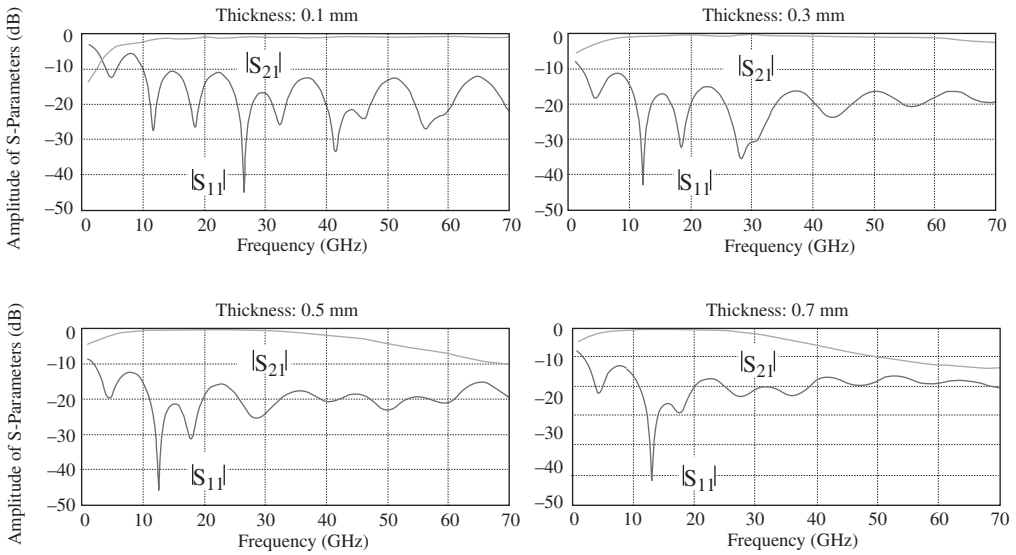


Figure 1.7 The comparison of $|S_{11}|$ and $|S_{21}|$ of a bent MS transmission-line on a LTCC board.

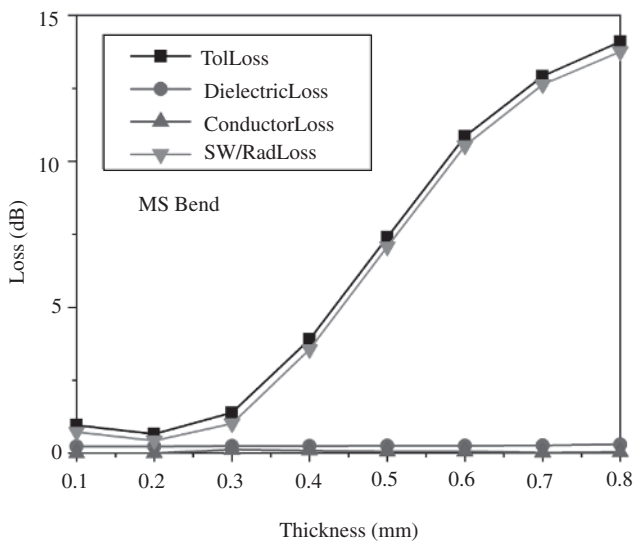


Figure 1.8 The main losses at 60 GHz of a bent MS transmission-line on a LTCC board with varying thickness.

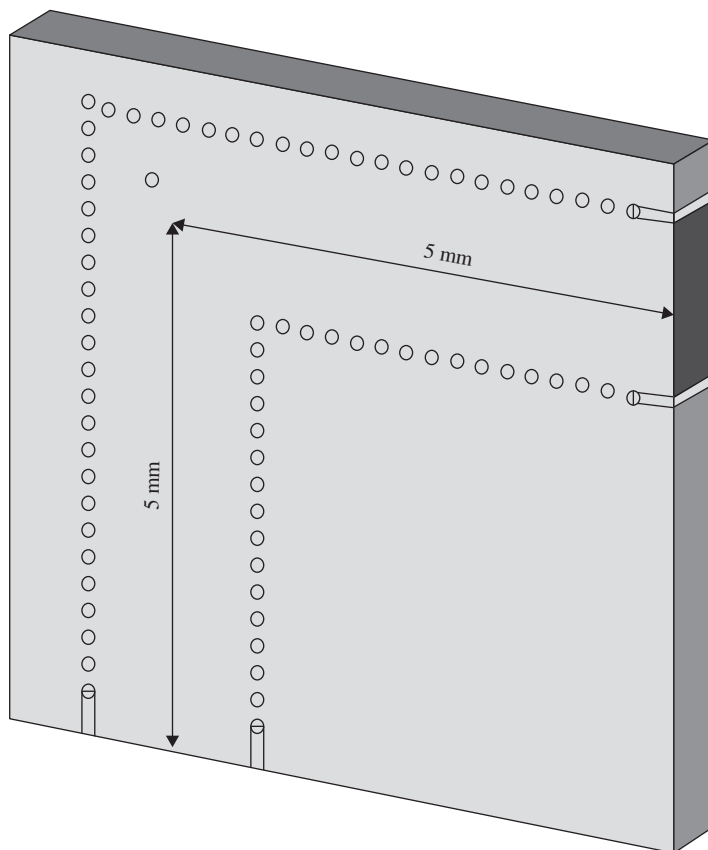


Figure 1.9 A 10-mm long bent SIW in a LTCC board.

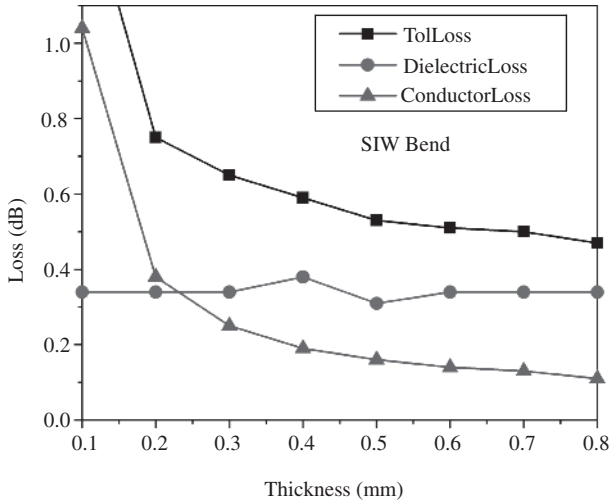


Figure 1.10 The main losses at 60 GHz of a bent SIW in a LTCC board with varying thickness.

In short, the SIW transmission line systems feature lower insertion loss at 60 GHz and above compared with the MS-lines suffering from several surface wave losses. However, it should be mentioned that the SIW has a more complicated fabrication and higher fabrication cost compared with the MS lines. The evaluation of performance and implementation cost is necessary to make a trade-off in the design.

1.8 Update of Millimeter Wave Technology in 5G NR and Beyond

Recently mmW has attracted much attention of the industry although it is not a new technology. In particular, the mobile communication networks are significantly increasing their capacity by increasing the usage efficiency of existing spectra such as massive multiple-input-multiple-output (massive MIMO), the number of small cell base stations, and the operating bandwidth by extending operating frequencies from sub-6 GHz bands to mmW bands to enhance the peak data rates of mobile broadband use case up to 20 Gbps in the downlink (DL) and 10 Gbps in the uplink (UL). With such high data rates, many new applications such as high-speed streaming of 4K or 8K UHD movies and self-driving cars will be supported.

According to the release of specifications by The 3rd Generation Partnership Project (3GPP), a standards organization developing the protocols for mobile telephony, the following bands as tabulated in Table 1.5 [53] have been defined for fifth-generation (5G) new radio (NR) networks. The allocated bandwidths reach up to 3 GHz each while the total frequency ranges from 24.25 to 40.00 GHz.

Table 1.6 compares the features of mobile communication network operating at 5G NR sub-6 GHz and mmW bands. Not surprisingly, the systems operating at mmW bands suffer from the higher path-loss and blocking due to weaker refraction and reflection in propagation in denser environments.

Based on the previous analysis and initial feedback from field trials, the mmW in 5G NR networks will have the typical applications as shown in Figure 1.11. It is estimated that for 5G NR the mmW systems can be used with the similar scenarios at sub-6 GHz bands, but coverage will be significantly reduced due to the higher path-loss and blocking of mmW propagation. The higher

Table 1.5 mmW frequency ranges for 5G NR (TDD).

NR operating band	$F_{UL/DL_low} - F_{UL/DL_high}$
n257	26.50–29.50 GHz
n258	24.25–27.50 GHz
n260	37.00–40.00 GHz

- Duplex Mode: Time-division duplexing (TDD)
- Uplink (UL): base station (BS) receive and user equipment (UE) transmit
- Downlink (DL): base station (BS) transmit and user equipment (UE) receive.

Table 1.6 Comparison of features of network at 5G NR sub-6 GHz and mmW bands.

	Sub-6 GHz	mmW
Bandwidth	~100 MHz	500 MHz @28 GHz/>2 GHz @E-band
BS/UE antenna configuration	Single/sectorized arrays	Very high-gain directional arrays
Network deployment	Low base-station density	Very high base-station density
Small-scale fading	Correlated with high rank	Correlated with low rank, varies with line-of-sight (LOS) or Non-LOS (NLOS)
Large-scale fading	Distance dependent path-loss	Distance dependent with random blockage model and total outage
No of users served simultaneously	High (>10)	Low (<10)

path-loss is caused by the reduced physical aperture of receive antennas with the same gain as the antennas operating at lower frequencies. Therefore, the electrical apertures or gain of the mmW antennas should be increased to keep the gain unchanged or link budget compared with the antennas operating at lower frequencies.

Besides the mmW frequency bands released by 3GPP for 5G NR, the extension of mmW bands from the lower edge frequencies around 30 to 60 GHz even higher has been proposed and investigated for mobile communication networks for years. However, due to even higher path-loss and severer blocking at upper mmW bands, the mmW systems may have different applications as shown in Figure 1.11. The systems operating at 60 GHz bands may be a good option for indoor hotspots or hot-region coverage for opportunistic connections and/or pointing connections for high data transmission. Systems operating at frequencies higher than typically 110 GHz have been used for long distance backhauls to replace higher cost optical fiber or cabled connections. The new application may be the backhauls between macro BSs and small cell BSs for low-cost and flexible network setup.

In short, it can be foreseen that the applications of mmW systems in the 5G NR are just a start and still present many technical challenges. In the 5G and even beyond 5G, the antenna technologies will play increasingly important roles. The small or compact multiple functional massive MIMO, beamforming/scanning, multi-beam, and reconfigurable antenna systems will be greatly developed to meet the challenging system demands.

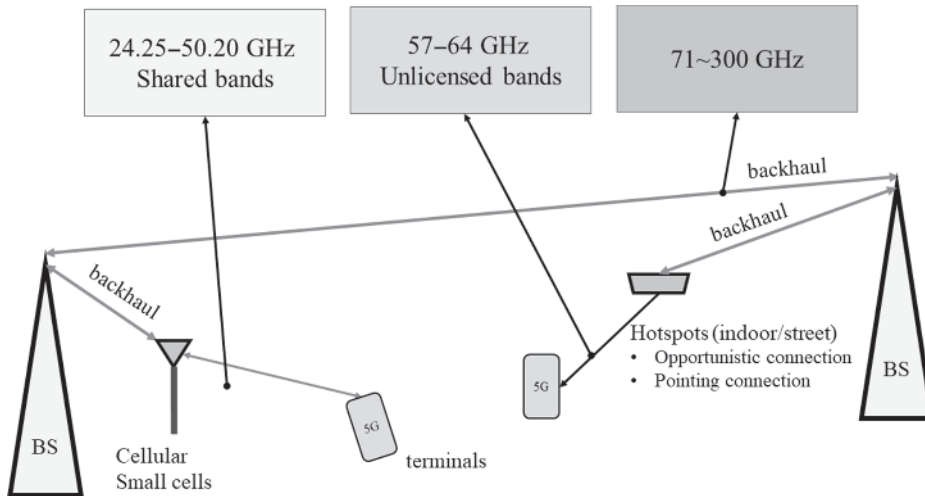


Figure 1.11 Potential mmW applications in 5G NR and future networks.

1.9 Organization of the book

This book is organized in the following way:

Chapter 1, “Introduction to Millimeter Wave Antennas” by Zhi Ning Chen, is an introductory chapter of this book. First the relevant concepts of mmW technology are introduced. Then the unique propagation characteristics of mmW are reviewed, associated with the existing and promising applications of mmW technologies. After that, the unique design challenges of antennas at mmW bands are addressed, followed by a brief overview of state-of-the-art mmW antenna designs. The last part briefly discusses the challenges in the fabrication of mmW antennas from the selection of materials to processes. The latest developments and applications of the mmW systems for 5G new radio and beyond are briefed for future research development of antenna technologies.

Chapter 2, entitled “Measurement Methods and Setups of Antennas at 60–325 GHz Bands” by Xianming Qing and Zhi Ning Chen introduces the testing setups of mmW antennas by addressing expensive testing setup, limited system dynamic range, complicated, and tedious calibration, as well as measurement procedures. This chapter deals with the measurement issues of the mmW antennas from 60 to 300 GHz. First, the state-of-the-art mmW antenna measurement systems are presented. Then the key considerations of configuring the measurement systems are addressed. In the last part, the detailed setup configurations for achieving the maximum system dynamic range with the available commercial accessories are described, wherein the measurement of reflection coefficient, gain, and radiation pattern of a number of antennas at 60, 140, and 270 GHz bands with different feeding connections (coax, waveguide, and probe) are exemplified.

In Chapter 3, “Substrate Integrated mmW Antennas on LTCC” Zhi Ning Chen and Xianming Qing introduce the basic concepts of SIW antennas, in particular, SIW slot antennas. Then, design examples in LTCC are elaborated. The examples include planar high-gain arrays operating at 60, 140, and 270 GHz. In particular, the three-dimensional corporate feeding network is introduced by taking advantage of the LTCC process.

In Chapter 4, “Broadband Metamaterial-Mushroom Antenna Array at 60 GHz Bands,” by Wei Liu and Zhi Ning Chen, the techniques for enhancing the bandwidth of patch antennas are reviewed first. Then, the bandwidth enhancement techniques are evaluated for substrates of high dielectric constant. In particular, the metamaterial mushroom antenna technique are introduced for the

LTCC mmW antenna design due to the merits of low profile, broadband, high gain, high radiation efficiency, low mutual coupling, and low cross-polarization levels.

Narrow-wall-fed Substrate integrated Cavity (SIC) Antenna at 60 GHz is discussed in Chapter 5, by Yan Zhang. This chapter addresses the unique challenges of mmW SIC antenna design. At first, the mmW cavity antennas are reviewed. Then, the selected state-of-the-art SIC antennas are introduced and discussed. In particular, the technique to excite an SIC using a narrow-wall slot is elaborated, and furthermore a 2×2 array with narrow-wall-slot fed SIW at 60 GHz is presented as an example.

Chapter 6, entitled “Cavity-Backed SIW Slot Antennas at 60 GHz,” by Ke Gong, introduces the history and milestones of the cavity-backed antennas (CBAs) first, together with some challenges for mmW applications. Then, the low-profile design methods and fabrication techniques about CBAs are analyzed, especially for the substrate integrated CBAs. After that, the low-profile SIW CBAs are reviewed. Their operating mechanisms are discussed, and methods for improving the performance, such as bandwidth enhancement, size reduction, and gain improvement, are presented. At last, a type of cavity-backed SIW slot antennas with big-aperture is presented as an example, with design details as a study case, including the antenna element. This type of antennas retains the advantage of conventional metallic CBAs, including high gain, high front-to-back ratio, and low cross-polarization level, and also keep the advantages of the planar antenna including low profile, light weight, low fabrication cost, and easy integration with the planar circuit.

In Chapter 7, “Circularly Polarized SIW Slot LTCC Antennas at 60 GHz,” Yue Li first reviews the selected state-of-the-art techniques for mmW circularly polarized (CP) antennas. Second, as a feasible example to achieve both wide impedance and axial ration (AR) bandwidths, an SIW-fed slot antenna array with strip loading is introduced at 60 GHz using an LTCC substrate. The AR bandwidth enhancement property is systematically described with the potential adoption in various mmW CP applications.

Chapter 8, entitled “Gain Enhancement of LTCC Microstrip Patch Antenna by Suppressing Surface Waves,” by Zhi Ning Chen and Xianming Qing, introduces the technology to suppress the surface wave losses caused by the thick and high-permittivity dielectric substrate in mmW antennas. First, the mechanism of generation of surface wave losses is discussed. Then the method to suppress the surface waves is addressed with an example of patch antenna. After that, the planar and via-less antenna array operating at 60 GHz is exemplified for gain enhancement by suppressing the surface wave losses. The method to suppress the surface wave is to cut open-air cavities around their radiating patches. The open-air cavities reduce the losses caused by severe surface waves and dielectric substrate at mmW bands. The arrays are excited through either a microstrip-line or stripline feed network with a grounded coplanar-waveguide (GCPW) transition. The GCPW transition is designed so that the antenna can be measured with the patch array facing free space, therefore reducing the effect of the probe station on the measurement. The proposed antenna arrays with the open-air cavities achieve gain enhancement of 1–2 dB compared with the conventional antenna array without any open-air cavity across the impedance bandwidth of about 7 GHz at the 60 GHz band.

In Chapter 9, “Substrate Integrated Antennas for Millimeter Wave Automotive Radars,” Xianming Qing and Zhi Ning Chen introduce the PCB-based high-gain substrate integrated mmW antennas for car radar sensors. First, the general aspects of automotive radar are addressed including the classification, the frequency band regulation, system requirements, and antenna design considerations. Second, the selected state-of-the-art antenna designs for 24-GHz and 77-GHz automotive radars are reviewed. After that, two types of antenna arrays are introduced. A compact co-planar waveguide (CPW) center-fed SIW slot antenna array is elaborated to achieve narrow H -plane beamwidth and low sidelobe levels for 24-GHz automotive radars. A transmit-array

on dual-layer PCB is introduced for automotive 77-GHz radar applications. With four SIW slot antennas as the primary feeds, the transmit-array is able to generate four switched beams. The coplanar structure significantly simplifies the transmit-array design and eases the fabrication, in particular, at mmW frequencies.

Chapter 10 is entitled “Sidelobe Reduction of Substrate Integrated Antenna Arrays at Ka-Band.” Teng Li first introduces the synthesis technologies of low sidelobe array factors and the optimization methods. To accurately get the desired pattern, a brief analysis of mutual coupling is presented. Then, the selected state-of-the-art feeding technology for SIW array antenna are reviewed. After that, the examples of the small array, monopulse array, and shaped beam array with sidelobe reduction and different feeding technologies are introduced for SIW array antenna at Ka-band.

In Chapter 11, “Substrate Edge Antennas,” Lei Wang and Xiaoxing Yin introduce substrate edge antennas (SEAs), which radiate from the edges of the PCBs. To diminish the mismatch between the PCB edge and the free space, two types of planar strips are printed in front of the SEA aperture. With the printed strips, both the impedance bandwidth and the front-to-back ratio are improved. Aiming at increasing the aperture efficiency, two kinds of substrate-integrated lenses are embedded in the SEAs. The phase-correcting lenses are integrated into the SEAs, maintaining the compact profiles of SEAs. Moreover, a leaky-wave SEA loaded with a prism lens is presented with a fixed-beam over a wide frequency band. The prism lens is implemented by utilizing a dispersive metasurface. By compensating for the dispersion of the leaky-wave SEA and the prism lens, fixed radiation beams are achieved over a 20% fraction bandwidth at Ka-band.

1.10 Summary

The research, development, and applications of mmW antennas have a long history. With the fast progress in device technologies and rapid deployment of system for a variety of commercial applications, theory, and technologies related to mmW antennas have been extensively investigated and developed [54–64]. This book will address the critical design challenges of mmW antennas for wireless communications and radar systems.

References

- 1 ITU-R Recommendation (2015). V.431: “Nomenclature of the frequency and wavelength bands used in telecommunications (Table I).” Geneva: International Telecommunication Union. https://www.itu.int/dms_pubrec/itu-r/rec/v/R-REC-V.431-8-201508-I!!PDF-E.pdf (accessed 19 December 2020).
- 2 Seybold, J.S. (2005). *Introduction to RF Propagation*, 3–10. Wiley.
- 3 Petty, K.R. and Mahoney, W.P. III, (2007). Weather applications and products enabled through vehicle infrastructure integration (VII). (Section 5) United States Department of Transportation – Federal Highway Administration Report No. FHWA-HOP-07-084. <https://ops.fhwa.dot.gov/publications/viirpt/viirpt.pdf> (accessed 19 December 2020).
- 4 Shannon, C.E. (1949). Communication in the presence of noise. *Proc. Inst. Rad. Eng.* 37 (1): 10–21.
- 5 Wiltse, J.C. (1984). History of millimeter and submillimeter waves. *IEEE Trans. Microwave Theory Tech.* 32 (9): 1118–1127.
- 6 Nichols, E.F. and Tear, J.D. (1923). Short electric waves. *Phys. Rev.* 21: 587–610.

- 7 Nichols, E.F. and Tear, J.D. (1923). Joining the infra-red and electric wave spectra. *Proc. Nat. Acad. Sci.* 9: 211–214.
- 8 Tear, J.D. (1923). The optical constants of certain liquids for short electric waves. *Phys. Rev.* 21: 611–622.
- 9 Cleeton, C.E. and Williams, N.H. (1934). Electromagnetic waves of 1.1cm wave-length and the absorption spectrum of ammonia. *Phys. Rev.* 45: 234–237.
- 10 Boot, H.A.H. and Randall, J.T. (1976). Historical notes on the cavity magnetron. *IEEE Trans. Electron Dev.* 23: 724–729.
- 11 Bennger, R. (1946). The absorption of one-half centimeter electromagnetic waves in oxygen. *Phys. Rev.* 70: 53–57.
- 12 Wartens, W.D. (1977). WT4 millimeter waveguide system: introduction. *Bell Syst. Tech. J.* 56: 1925–1928.
- 13 Button, K.J. and Wiltse, J.C. (eds.) (1981). *Millimeter Systems*, vol. 4, (series on Infrared and Millimeter Waves). NY: Academic.
- 14 Schwartz, R.F. (1954). Bibliography on directional couplers. *IRE Trans. Microwave Theory Tech.* 2: 58–63.
- 15 Convert, G., Yeou, T., and Pasty, B. (1959). Millimeter-wave O-carcinotron. In: *Proceedings of Symposium on Millimeter Waves*, vol. IX, 313–339.
- 16 Wiltse, J.C. (1959). Some characteristics of dielectric image lines at millimeter wavelengths. *IRE Trans.* 7: 63–69.
- 17 Taub, J.J., Hindin, H.J., Hinckelmann, O.F., and Wright, M.L. (1963). Submillimeter components using oversized quasi-optical waveguide. *IEEE Trans. Microwave Theory Tech.* 11 (9): 338–345.
- 18 Richer, K.A. (1974). Near earth millimeter-wave radar and radiometry. *Proc. IEEE Int. Symp. Microw. Theory Tech.*: 470–474.
- 19 Wiltse, J.C. (1979). Millimeter wave technology and applications. *Microw. J.* 22: 39–42.
- 20 Chang, K. and Sun, C. (1983). Millimeter-wave power-combining techniques. *IEEE Trans. Microwave Theory Tech.* 31 (2): 91–107.
- 21 Chen, Z.N. (ed.) (2016). *Handbook of Antenna Technologies*. Springer.
- 22 Balanis, C.A. (2016). *Antenna Theory: Analysis and Design*, 4e. Wiley.
- 23 Uchimura, H., Takenoshita, T., and Fujii, M. (1998). Development of a “laminated waveguide”. *IEEE Trans. Microwave Theory Tech.* 46 (12): 2438–2443.
- 24 Takenoshita, T. and Uchimura, H. (1999). Laminated aperture antenna and multilayered wiring board comprising the same. EP20030026894 (Application number in 1998) and EP0893842B1 (Grant number in 2004). <https://patentimages.storage.googleapis.com/74/5e/eb/c2c2e031af31c7/EP0893842A2.pdf> (accessed 19 December 2020).
- 25 Hirokawa, J. and Ando, M. (1998). Single-layer feed waveguide consisting of posts for plane TEM wave excitation in parallel plates. *IEEE Trans. Antennas Propag.* 46 (5): 625–630.
- 26 Deslandes, D. and Wu, K. (2001). Integrated microstrip and rectangular waveguide in planar form. *IEEE Microwave Wirel. Compon. Lett.* 11 (2): 68–70.
- 27 Yan, L., Hong, W., Hua, G. et al. (2004). Simulation and experiment on SIW slot array antennas. *IEEE Microwave Wirel. Compon. Lett.* 14 (9): 446–448.
- 28 Sebastian, M.T., Uvic, R., and Jantunen, H. (eds.) (2017). *Microwave Materials and Applications*. Wiley.
- 29 Sebastian, M. and Jantunen, H. (2008). Low loss dielectric materials for LTCC applications. *Int. Mat. Rev.* 53 (2): 57–90.
- 30 Ullah, U., Ain, M.F., Mahyuddin, N.M. et al. (2015). Antenna in LTCC technologies: a review and the current state of the art. *IEEE Antennas Propag. Mag.* 57 (2): 241–260.

- 31 Deslandes, D. and Wu, K. (2006). Accurate modeling, wave mechanisms, and design considerations of a substrate integrated waveguide. *IEEE Trans. Microwave Theory Tech.* 54 (6): 2516–2526.
- 32 She, Y., Tran, T.H., Hashimoto, K. et al. (2011). Loss of post-wall waveguides and efficiency estimation of parallel-plate slot arrays fed by the post-wall waveguide in the millimeter-wave band. *IEICE Trans. Electron.* E94-C (3): 312–320.
- 33 Gatti, F., Bozzi, M., Perregrini, L. et al. (2006). A novel substrate integrated coaxial line (SICL) for wideband applications. In: *Proceedings of the 36th European Microwave Conference*, 1614–1617.
- 34 Shao, Y., Li, X.-C., Wu, L.-S., and Mao, J.-F. (2017). A wideband millimeter-wave substrate integrated coaxial line array for high-speed data transmission. *IEEE Trans. Microwave Theory Tech.* 65 (8): 2789–2800.
- 35 Zhu, F., Hong, W., Chen, J.-X., and Wu, K. (2012). Ultra-wideband single and dual baluns based on substrate integrated coaxial line technology. *IEEE Trans. Microwave Theory Tech.* 60 (10): 3062–3070.
- 36 Yang, T.Y., Hong, W., and Zhang, Y. (2016). An SICL-excited wideband circularly polarized cavity-backed patch antenna for IEEE 802.11aj (45 GHz) applications. *IEEE Antennas Wirel. Propag. Lett.* 15: 1265–1268.
- 37 Liu, B., Xing, K.J., Wu, L. et al. (2017). A novel slot array antenna with substrate integrated coaxial line technique. *IEEE Antennas Wirel. Propag. Lett.* 16: 1743–1746.
- 38 Miao, Z.-W. and Hao, Z.-C. (2017). A wideband reflectarray antenna using substrate integrated coaxial true-time delay lines for QLink-pan applications. *IEEE Antennas Wirel. Propag. Lett.* 16: 2582–2585.
- 39 Xing, K., Liu, B., Guo, Z. et al. (2017). Backlobe and sidelobe suppression of a Q-band patch antenna array by using substrate integrated coaxial line feeding technique. *IEEE Antennas Wirel. Propag. Lett.* 16: 3043–3046.
- 40 Liang, W. and Hong, W. (2012). Substrate integrated coaxial line 3 dB coupler. *IET Electron. Lett.* 48 (1): 35–36.
- 41 Chu, P. et al. (2014). Wide stopband bandpass filter implemented with spur stepped impedance resonator and substrate integrated coaxial line technology. *IEEE Microwave Wirel. Compon. Lett.* 24 (4): 218–220.
- 42 Zhang, J., Zhang, X., and Shen, D. (2016). Design of substrate integrated gap waveguide. *IEEE MTT-S Int. Microwave Symp. Dig.*: 1–4.
- 43 Zhang, J., Zhang, X., Shen, D., and Kishk, A.A. (2017). Packaged microstrip line: a new quasi-TEM line for microwave and millimeter-wave applications. *IEEE Trans. Microwave Theory Tech.* 65 (3): 707–718.
- 44 Cao, B., Wang, H., Huang, Y., and Zheng, J. (2015). High-gain L-probe excited substrate integrated cavity antenna array with LTCC-based gap waveguide feeding network for W-band application. *IEEE Trans. Antennas Propag.* 63 (12): 5465–5474.
- 45 Cao, B., Wang, H., and Huang, Y. (2016). W-band high-gain TE₂₂₀ -mode slot antenna array with gap waveguide feeding network. *IEEE Antennas Wirel. Propag. Lett.* 15: 988–991.
- 46 Dadgarpour, A., Sorkherizi, M.S., and Kishk, A.A. (2016). Wideband low-loss magnetoelectric dipole antenna for 5G wireless network with gain enhancement using meta lens and gap waveguide technology feeding. *IEEE Trans. Antennas Propag.* 64 (12): 5094–5101.
- 47 Sorkherizi, M.S., Dadgarpour, A., and Kishk, A.A. (2017). Planar high-efficiency antenna array using new printed ridge gap waveguide technology. *IEEE Trans. Antennas Propag.* 65 (7): 3772–3776.

- 48 Bayat-Makou, N. and Kishk, A. (2017). Millimeter-wave substrate integrated dual level gap waveguide horn antenna. *IEEE Trans. Antennas Propag.* 65 (12): 6847–6855.
- 49 Dadgarpour, A., Sorkherizi, M.S., Denidni, T.A., and Kishk, A.A. (2017). Passive beam switching and dual-beam radiation slot antenna loaded with ENZ medium and excited through ridge gap waveguide at millimeter-waves. *IEEE Trans. Antennas Propag.* 65 (1): 92–102.
- 50 Zhang, J., Zhang, X., and Kishk, A.A. (2018). Broadband 60 GHz antennas fed by substrate integrated gap waveguides. *IEEE Trans. Antennas Propag.* 66 (7): 3261–3270.
- 51 Shen, D., Ma, C., Ren, W. et al. (2018). A low-profile substrate-integrated-gap-waveguide-fed magnetoelectric dipole. *IEEE Antennas Wirel. Propag. Lett.* 17: 1373–1376.
- 52 Yeap, S.B., Chen, Z.N., Li, R. et al. (2012). 135-GHz co-planar patch array on BCB/silicon with polymer-filled cavity. *Int. Workshop Antennas Tech.*: 1–4.
- 53 3GPP TS 38.101–2 v15.2, online available: <https://www.3gpp.org> (accessed 19 December 2020).
- 54 Chen, Z.N., Chia, M.Y.W., Gong, Y. et al. (2011). Microwave, millimeter wave, and Terahertz technologies in Singapore. In: *Proceedings of the 41st European Microwave Conference*, 1–4.
- 55 Chen, Z.N. et al. (2012). Research and development of microwave & millimeter-wave technology in Singapore. In: *Proceedings of the 42nd European Microwave Conference*, 1–4.
- 56 Li, T., Meng, H.F., and Dou, W.B. (2014). Design and implementation of dual-frequency dual-polarization slotted waveguide antenna array for Ka-band application. *IEEE Antennas Wirel. Propag. Lett.* 13: 1317–1320.
- 57 Mao, C.-X., Gao, S., Luo, Q. et al. (2017). Low-cost X/Ku/Ka-band dual-polarized array with shared-aperture. *IEEE Trans. Antennas Propag.* 65 (7): 3520–3527.
- 58 Wang, Z., Xiao, L., Fang, L., and Meng, H. (2014). A design of E/Ka dual-band patch antenna with shared aperture. In: *Proceedings of the Asia-Pacific Microwave Conference*, 333–335.
- 59 Han, C., Huang, J., and Chang, K. (2005). A high efficiency offset-fed X/Ka-dual-band reflectarray using thin membranes. *IEEE Trans. Antennas Propag.* 53 (9): 2792–2798.
- 60 Hsu, S.-H., Han, C., Huang, J., and Chang, K. (2007). An offset linear-array-fed Ku/Ka dual-band reflectarray for planet cloud. *IEEE Trans. Antennas Propag.* 55 (11): 3114–3122.
- 61 Chaharmir, M. and Shaker, J. (2015). Design of a multilayer X-/Ka-band frequency-selective surface-backed reflectarray for satellite applications. *IEEE Trans. Antennas Propag.* 63 (4): 1255–1262.
- 62 Attia, H., Abdelghani, M.L., and Denidni, T.A. (2017). Wideband and high-gain millimeter-wave antenna based on FSS Fabry–Perot cavity. *IEEE Trans. Antennas Propag.* 65 (10): 5589–5594.
- 63 Li, T. and Chen, Z.N. (2020). Wideband Sidelobe-level reduced Ka-band Metasurface antenna Array fed by substrate integrated gap waveguide using characteristic mode analysis. *IEEE Trans. Antennas Propag.* 68 (3): 1356–1365.
- 64 Hong, W. et al. (2017). Multibeam antenna technologies for 5G wireless communications. *IEEE Trans. Antennas Propag.* 65 (12): 6231–6249.